

Unsupervised Adaptation of Semantic Segmentation Models without Source Data

Sujoy Paul, Ansh Khurana, Gaurav Aggarwal
Google Research

{sujoy, anshkhurana, gauravaggarwal}@google.com

Abstract

We consider the novel problem of unsupervised domain adaptation of source models, without access to the source data for semantic segmentation. Unsupervised domain adaptation aims to adapt a model learned on the labeled source data, to a new unlabeled target dataset. Existing methods assume that the source data is available along with the target data during adaptation. However, in practical scenarios, we may only have access to the source model and the unlabeled target data, but not the labeled source, due to reasons such as privacy, storage, etc. In this work, we propose a self-training approach to extract the knowledge from the source model. To compensate for the distribution shift from source to target, we first update only the normalization parameters of the network with the unlabeled target data. Then we employ confidence-filtered pseudo labeling and enforce consistencies against certain transformations. Despite being very simple and intuitive, our framework is able to achieve significant performance gains compared to directly applying the source model on the target data as reflected in our extensive experiments and ablation studies. In fact, the performance is just a few points away from the recent state-of-the-art methods which use source data for adaptation. We further demonstrate the generalisability of the proposed approach for fully test-time adaptation setting, where we do not need any target training data and adapt only during test-time.

1. Introduction

Deep neural networks have shown immense success for dense prediction tasks, such as semantic segmentation [5]. However, models learned on one dataset, say the source, may not generalize well to a new dataset, say the target. Annotating every new target dataset is expensive, especially for the semantic segmentation task. For example, a single image from the Cityscapes dataset required about 1.5 hours to annotate [9]. To avoid the requirement of annotated target data, Unsupervised Domain Adaptation (UDA) methods [15, 52] adapt the model learned with labeled source data to the target dataset, without needing annotated target images.

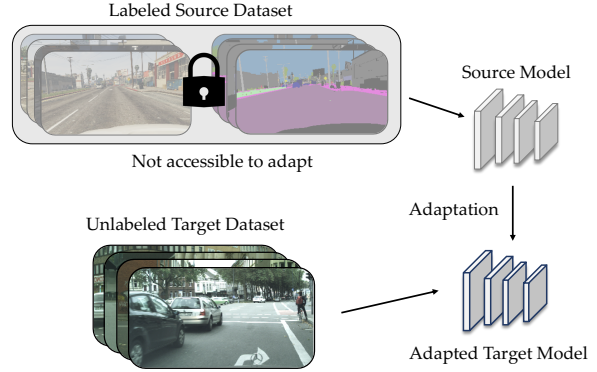


Figure 1. **Overview.** Unsupervised domain adaptation methods for semantic segmentation in literature use labeled source dataset while adapting to an unlabeled target dataset. However, in this work, we only use the knowledge from the source model for adaptation without access to the source data.

In the literature, UDA methods for semantic segmentation assume that data points from both the source and the target datasets are available for adaptation. However, such an assumption may not be practical, where either the source dataset cannot be shared to maintain privacy or the source dataset may take up a lot of storage space. In this case, one has access to only the light-weight source model which was trained using labeled source data. This would restrict sharing private information as well as require much less storage. For example, storing the GTA5 dataset [40] used as source in most UDA methods, needs 57 GB of storage whereas a model trained using the same data requires only 0.17 GB. With this motivation, in this work, we do not assume access to any source data and adapt the source model using only the unlabeled target data for semantic segmentation. Figure 1 illustrates the problem pictorially.

Before diving into the details of source-free adaptation, let's study the techniques used in UDA for semantic segmentation using source data. They can be categorized mainly into three groups: 1) output space adaptation [16, 50] that aligns the source and target output distributions, 2) pixel space adaptation [8, 15] that translates the source image dis-

tribution to the target distribution, and uses them for training, and finally, 3) pseudo labeling [26,66] that predicts the labels of the target images using the source model and uses them for training. When we do not have access to the source data, the first two methods are not even applicable. Recent methods on UDA for classification task [27,60] without source data largely follow the third strategy, i.e., pseudo-labeling. A few methods in this line of work also generate data from the target distribution to boost the performance [23]. Very recently published works [28,42] for source-free adaptation of segmentation models are no different. Additionally, [28] also follow the first option by dividing the target data into easy (source) and hard (target) group and train an additional discriminator.

In this work, we propose a novel consistency based self-training approach to adapt the source model using unlabeled target images. As the target data comes from a shifted distribution than the source, we first update the norm parameters of the network using the unlabeled target data. Then, we extract knowledge from the source model by pseudo-labeling the unlabeled target. The extracted pseudo-labels should be consistent against certain spatial transformations on images such as rotation, flipping, mirroring, and image augmentations such as cutout, Gaussian blur, etc. We use these consistencies to enhance the knowledge extracted from the source model. This can be posed as a constrained optimization problem, where in each iteration, we first compute the gradients of the target model using the actual pseudo-labels with respect to the source model, and then obtain the gradients using the consistency losses computed with respect to the current target model. We show via empirical analysis that these simple consistencies with pseudo-labeling help to considerably improve the performance of the model on the target images. We also create a pseudo image distribution by collaging pairs of images, which enhances the variety of images in the dataset, and helps to regularize the model.

We evaluate our framework on three different settings: GTA5 \rightarrow Cityscapes and SYNTHIA \rightarrow Cityscapes for outdoor scenes and the novel setting of SceneNet \rightarrow SUN for indoor scenes, showcasing the generic nature of our algorithm. There is no known effort in the literature to show domain adaptation results on the mentioned indoor setting. Further, to demonstrate the generalisability of our consistency based approach, we apply it in the fully test-time adaptation setting [55], where it outperforms loss functions proposed by recent methods dedicated for fully test time adaptation [35,55] on all the above three dataset settings. The **main contributions** of our work are:

- We tackle the interesting problem of source-free adaptation for semantic segmentation and propose a self-training approach by imposing certain input-output consistencies to extract the knowledge from the source model.
- Empirical analysis shows that our method establishes the new state-of-the-art for source-free adaptation, and is only a few points away from the state-of-the-art which uses the entire labeled source dataset to adapt.
- Our method works well even for test time adaptation, where we do not access even the unlabeled target, and the adaptation is done individually for each test sample.

2. Related Works

We divide the related works discussion in two parts: 1) methods using the source data to adapt (most works in literature), and 2) methods that do not use any source data, (a few recent efforts, mostly for classification and a couple for the segmentation task).

UDA with Source Data. UDA methods for the image classification task aim to align the source and target distributions. To do so, maximum mean discrepancy [29] and adversarial learning [13,52] based approaches have been proposed. A few algorithms focus on improving deep models [10,21,30,43] and translating the input source images to the target domain [2,15,49]. For the more challenging task of semantic segmentation, existing UDA methods can be categorized primarily into three groups: output alignment, pixel-adaptation and pseudo-labeling. In output alignment, the methods aim at aligning the output or feature distribution between the source and target domains [1,6,7,16,50,64]. For pixel alignment, similar to as in image classification, the algorithms translate the input images to the target domain by changing style, while preserving content information [4,8,15,36,57,59,65]. For pseudo-labeling, methods aim to generate pixel-wise pseudo labels on the target images, which is utilized to fine-tune the segmentation model trained on the source [11,22,26,34,38,44,45,63,66]. There are also several methods in literature that try to combine these strategies [12,17,19,25,31,37,39,47,51,54,56]. Compared to these approaches, we assume no access to the source dataset, which is a more realistic setting but makes the task much more challenging.

UDA without Source Data. Unlike the above methods, there have been a few works for classification tasks which do not use source data, but only the source model for adaptation. The methods involve - entropy minimization with divergence maximization [27], pseudo-labeling with self-reconstruction [60], generating additional target images [23] and self-supervision [58]. For source-free adaptation for semantic segmentation, recently, [28] proposed an algorithm that combines ideas from the above methods like image generation, pseudo-labeling and output space adaptation by dividing the target into easy and hard, and learning an additional discriminator to align them. In [42], pseudo-labeling and robustness to dropout randomness is used to tackle the

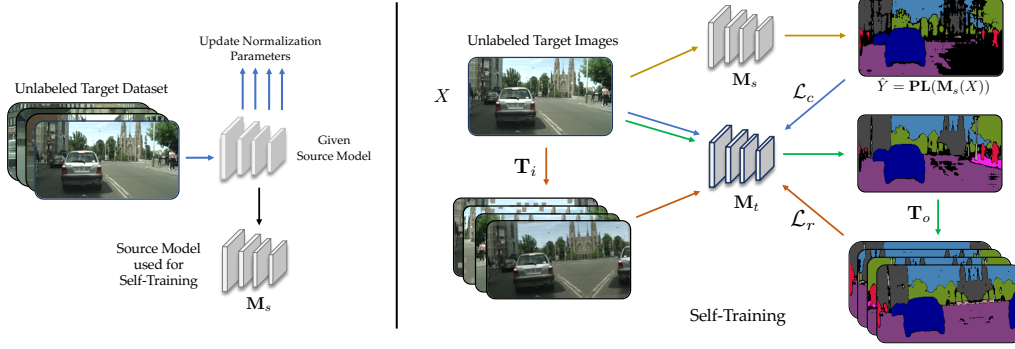


Figure 2. **Framework overview.** (Left) Given the source model, we first update the norm parameters of the network by just forward propagating the unlabeled target images, to obtain the model M_s . (Right) Then we learn a new target model M_t using self-training. We first obtain the pseudo-labels using M_s and compute the classification loss \mathcal{L}_c . Then, we transform the input image (T_i) as well as the target model’s prediction (T_o) in the current iteration and impose certain consistencies via the loss function \mathcal{L}_r . On the right-hand side, each arrow color denotes one full pass, either forward or forward+backward propagation.

problem, which performs very similar to our strong baseline of Pseudo-Label (PL). Pseudo-Labeling is also used in [61] with the concept of negative learning, i.e., the pixels where the model is not confident towards a certain positive label, it may be confident towards multiple negative labels. Very recently, a method for robust training of source models is proposed in [20], followed by pseudo-labeling on the target. In comparison to this method, we do not assume access to the source data or training process but only the trained source model.

3. Domain Adaptation from Source Models

In this section, we formally define the problem statement, followed by an overview of our framework, and finally a detailed description of each blocks in our framework.

3.1. Problem Statement

Consider that we have a source model for semantic segmentation, which needs to be adapted to a new target domain, given only unlabeled target images, without access to the source images on which the source model was trained. Formally, consider we have a source model $M_s : \mathbb{R}^{H \times W \times 3} \rightarrow \mathbb{R}^{H \times W \times C}$, which takes as input an RGB image and predicts for every pixel its category. H, W are the height and width of the image and C is the number of categories/labels. Now, given an unlabeled target dataset, $\mathcal{D}_t = \{X_i\}_{i=1}^n$, our goal is to adapt the source model M_s to a new model M_t , such that it performs better on images drawn from the target distribution, than directly using the source model on the target images.

3.2. Overall Framework

An overview of our proposed framework is presented in Figure 2. As the target images come from a different

distribution than what the source model is trained with, we first update only the norm parameters of the network, i.e., mean and variance of BatchNorm or InstanceNorm, by just forward propagating the target domain images \mathcal{D}_t through the given source model. This does not change the network weights, but only the norm parameters are updated. After that, we use the updated source model M_s to pseudo-label the target images only for the confident pixels. Along with these pseudo-labels, we impose two different types of consistency constraints using augment and spatial transformations. This helps to efficiently extract knowledge from the source model that in turn helps the adapted model perform better on the target images. Additionally, we create a pseudo image distribution by collaging pairs of images, thus creating a wider variety of image compared to the target dataset. We learn a new target model M_t by simultaneously optimizing for the pseudo-labels with the consistency constraints.

3.3. Update Normalization Parameters

BatchNorm [18] and InstanceNorm [53] are commonly used in deep neural networks to avoid over-fitting, stabilize training, and faster convergence. For every activation layer in the network, these normalization methods estimate two parameters during training, viz., the mean and variance, which are then used in the testing phase. However, these parameters are only a good estimate for the images in the training distribution. Thus, in domain adaptation, where the target data may belong to a different distribution than the source, it may be useful to first update the mean and variance of the normalization layers, using the unlabeled target data. This is inspired by works in literature [3, 24] where they estimate domain-specific normalization parameters, while having access to both the source and the target data, during training.

In order to update the normalization statistics, we only

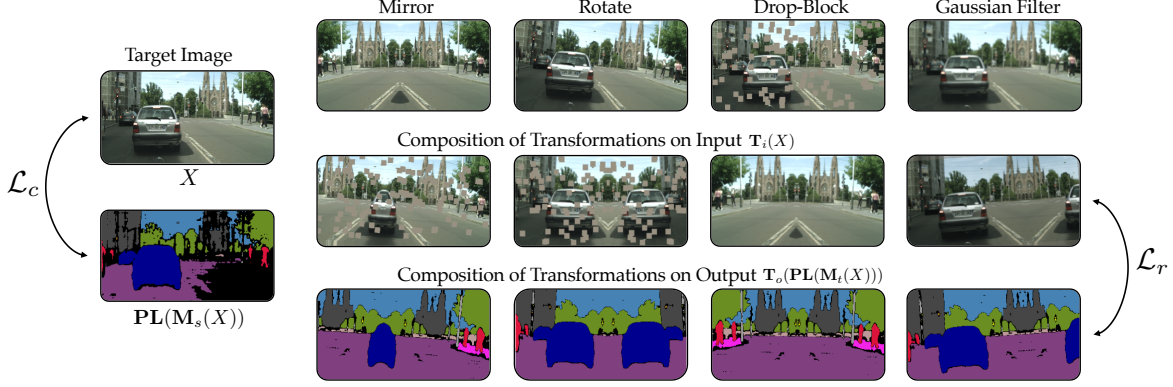


Figure 3. **Transforms.** This figure shows the different transforms used in our algorithm. The left-most side shows an image with the pseudo-labels obtained from the source model M_s , which are used to compute the loss \mathcal{L}_c . The top row shows the transformations individually, followed by their random compositions in the second row, and the last row shows the transformations on the output of the target model for a certain iteration, which are used a ground-truth for computing loss \mathcal{L}_r .

forward propagate the unlabeled target images through the network for one epoch and use the following update rule for a particular layer in each iteration.

$$\mu \leftarrow (1 - 1/i)\mu + \frac{1}{i}\mu_i \quad (1)$$

$$\sigma^2 \leftarrow (1 - 1/i)\sigma^2 + \frac{1}{i}\sigma_i^2 \quad (2)$$

where $i = \{1, \dots, n\}$. μ_i and σ_i^2 are the mean and variance of that layer with X_i as input. Note that we use instance normalization in all our experiments. This is because in semantic segmentation, to handle high resolution images, the batch size can typically only be one. Further, to estimate the mean and variance on the new target data, we need to forward propagate each target image only once, without any backward propagation. This step only updates the normalization parameters, mean and variance, and not the weights of the network. We call this updated model M_s , which we use to learn the target model M_t , as discussed next.

3.4. Pseudo-Labeling with Constraints

Given the normalization updated source model M_s , we use it to label the target images via confidence-filtered pseudo labeling. Additionally, we impose consistency using certain transforms, which gives the model an opportunity to improve beyond learning from just the pseudo-labeled dataset.

3.4.1 Pseudo-Labeling:

The pseudo-labeling function $\hat{Y} = \text{PL}(M(X))$ to label an image X with a model M can be defined as follows:

$$\hat{Y}^{x,y} = \begin{cases} j^* = \arg \max_j [M(X)]^{x,y}, & \text{if } \max_j [M(X)]^{x,y} > p_{j^*} \\ \text{No Label}, & \text{otherwise} \end{cases} \quad (3)$$

where the superscript x, y , represents the spatial co-ordinates, $j \in \{1, \dots, C\}$, and $[M(X)]^{x,y}$ is a C -dimensional vector summing to 1, representing the pixel's prediction. p_j is the threshold for prediction confidence of label j , which will be discussed in more detail subsequently. We label the unlabeled target dataset \mathcal{D}_t using the pseudo-labeling function to obtain a new dataset $\hat{\mathcal{D}}_t = \{X_i, \hat{Y}_i\}_{i=1}^n$, where $\hat{Y}_i = \text{PL}(M_s(X_i))$.

We can train a new model M_t using the pseudo-labeled set $\hat{\mathcal{D}}_t$, which would reduce the uncertainties in the source model M_s , offering a better hypothesis on the target. However, the model can only be as good as the pseudo-labels, without much room for improvement. We observe that certain transforms on the target input actually lead to undesirable changes in the output. Thus, we constrain these to desirable outputs, which acts as a signal to improve beyond the pseudo-labeled set.

3.4.2 Consistency as Constraint

The target network learned using the pseudo labels from Eqn. 3 can only be as good as the pseudo-labels and it may overfit to that particular set $\hat{\mathcal{D}}_t$. Because of this, we observe that under certain transformations to the input image such as cutout, Gaussian blur, image rotation, image mirroring, etc., the network does not predict consistent labels. By consistent, we mean labels similar to what one would obtain without applying these transformations. This observation motivates us to use this consistency as constraint while learning from the pseudo-labeled dataset $\hat{\mathcal{D}}_t$, which acts as an additional signal to improve beyond pseudo-labeling. We use two different types of image transformations namely - augment and spatial transforms, as discussed next. Moreover, we create additional images (collages) by joining pairs of images and apply similar consistency constraints to further enhance

the model.

Augment Transforms (\mathcal{T}_a): Cutout and Gaussian blur belong to this transform, as shown in Figure 3. In this case, we constrain the output to be similar even after applying these transforms, i.e., if we consider a transform $\mathbf{T} \in \mathcal{T}_a$, then the consistency constraint can be expressed as

$$\mathbf{M}_t(\mathbf{T}(X)) \approx \mathbf{M}_t(X) \quad (4)$$

In cutout, we randomly choose k blocks of size $b \times b$ from the image, and set them to 0, where $\frac{kb^2}{HW} \approx p$, with two free parameters b, p . H and W are the image height and width. For Gaussian blur, we choose a kernel size and filter variance. Please refer to the appendix for details on the parameter values used for these transformations (Figure 6).

Spatial Transforms (\mathcal{T}_s): Image mirroring and rotation fall under this transform set as shown in Figure 3. Compared to augmentations, in this case, the output should not be the same as obtained from the original image, but should also be transformed. Formally, considering a transformation $\mathbf{T} \in \mathcal{T}_s$, the consistency constraint can be expressed as

$$\mathbf{M}_t(\mathbf{T}(X)) \approx \mathbf{T}(\mathbf{M}_t(X)) \quad (5)$$

Note that the order of the model and transform is switched in this case. For image mirroring, we first randomly choose a column, vertically splitting the image, and mirror the larger side of the image onto the smaller side. For rotation, we randomly choose the rotation degree between $[-5^\circ, +5^\circ]$.

Learning from Image Collages. Mixup [62] uses weighted combination of image pairs and their labels to regularize model training. Motivated by this, we propose to combine two images into a single image, but in the spatial domain, as shown in Figure 4. Given a pair of images X_i, X_j , the collage image is constructed by concatenating the first half of X_i with the second half of X_j along the width. Now, to obtain the pseudo-labels for the collage image, we also concatenate the pseudo-labels $\mathbf{PL}(\mathbf{M}_s(X_i))$ and $\mathbf{PL}(\mathbf{M}_s(X_j))$, as shown in Figure 4. Note that in our algorithm, we learn only from these collage images, and X from here onwards denotes these collage images. This creates a wider variety of images that helps to improve the target model.

Optimization Problem: Using these consistency constraints, we solve the following optimization problem:

$$\min_{\mathbf{M}_t} \mathcal{L}_c = \sum_{X \in \mathcal{D}_t} l_c(\mathbf{M}_t(X), \mathbf{PL}(\mathbf{M}_s(X))) \quad (6)$$

$$\text{s.t. } \mathbf{M}_t(\mathbf{T}(X)) \approx \mathbf{M}_t(X) \quad \forall X \in \mathcal{D}_t, \mathbf{T} \in \mathcal{T}_a \quad (7)$$

$$\mathbf{M}_t(\mathbf{T}(X)) \approx \mathbf{T}(\mathbf{M}_t(X)) \quad \forall X \in \mathcal{D}_t, \mathbf{T} \in \mathcal{T}_s \quad (8)$$

The objective function is thus to optimize for the pseudo-labels for the confident pixels as obtained from Eqn. 3 using

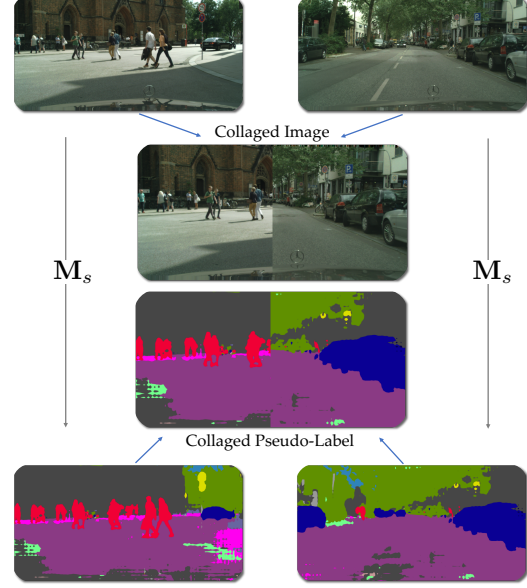


Figure 4. Process of image and pseudo-label collage creation. We use such collages to learn the target model.

cross-entropy loss l_c , such that the output of the target model is consistent with augment and spatial transforms. In practice, we compose the two sets of transforms to strengthen its power. To do so, in each iteration, we randomly choose a set of transformations $\mathcal{T} = \{\mathbf{T}_0, \dots, \mathbf{T}_k\} \in \mathcal{P}(\mathcal{T}_a \cup \mathcal{T}_s) \setminus \emptyset$. Due to the differences in the consistencies, the transforms need to be composed differently for input and output. The input transform is a composition of all the transforms, $\mathbf{T}_i = \mathbf{T}_0 \circ \dots \circ \mathbf{T}_k$. But to compose the output transform, we remove those drawn from \mathcal{T}_a , and then compose the rest in the same manner as input transform to obtain \mathbf{T}_o . Then, the constraints can be simplified as $\mathbf{M}_t(\mathbf{T}_i(X)) \approx \mathbf{T}_o(\mathbf{M}_t(X))$.

We approximate the constraint using two losses, and impose it via the penalty method. For every iteration, we consider $\mathbf{T}_o(\mathbf{M}_t(X))$ i.e., the transformed outputs from the current iteration target model, as ground-truths for the losses, and do not pass gradients through it, as otherwise trivial solutions can satisfy the constraints. The two losses are:

$$\mathcal{L}_r = \sum_{X \in \mathcal{D}_t} l_c(\mathbf{M}_t(\mathbf{T}_i(X)), \mathbf{T}_o(\mathbf{M}_t(X))) + l_c(\mathbf{M}_t(\mathbf{T}_i(X)), \mathbf{T}_o(\mathbf{PL}(\mathbf{M}_t(X)))) \quad (9)$$

where l_c is the cross-entropy loss. The first loss is a form of soft pseudo-labeling and computed for every pixel, whereas the second loss is hard pseudo-labeling, which only computes the loss for the confident pixels.

Parameter Updates. We optimize using Stochastic Gradient Descent. Note that we use the pseudo-labels using \mathbf{M}_s for ground-truth in the loss function of Eqn. 6 and \mathbf{M}_t in the

current iteration as the ground-truth for the loss function in Eqn. 9. For clarity, the SGD updates for the k^{th} iteration, with η as the learning rate can be expressed as follows:

$$\mathbf{M}_t^{k+1} = \mathbf{M}_t^k - \eta \nabla_{\mathbf{M}_t} (\mathcal{L}_c(\mathbf{M}_s) + \mathcal{L}_r(\mathbf{M}_t^k)) \quad (10)$$

where the argument in the brackets represent the models used to obtain the ground truths to compute the losses.

Pseudo-label Thresholds. To obtain the pseudo-labels using the source model \mathbf{M}_s , we set the thresholds to be $\min(0.9, \text{median of label-wise confidence})$, where the median is computed over all pixel predictions of the dataset for that label. The confidence distribution varies across labels, which motivates us to choose a label-dependent threshold rather than a fixed threshold for all labels. This strategy is commonly used in literature, and we also observe a boost in performance using this strategy. Now, as the target model \mathbf{M}_t evolves over time, we do not keep the same threshold to obtain the pseudo-label for its predictions, but rather update it using exponential moving average as follows:

$$\mathbf{p} = \lambda \mathbf{p} + (1 - \lambda) \mathbf{p}_k \quad (11)$$

where \mathbf{p} is the threshold vector over the C categories and used for the target model, \mathbf{p}_k is the threshold vector obtained for the image in the k^{th} iteration using the median strategy mentioned above, computed over all pixel predictions of that image for that label.

4. Experiments

Datasets: We evaluate our framework on three combinations of source \rightarrow target datasets covering both outdoor and indoor scenes. For outdoor, we evaluate on GTA5 [40] \rightarrow Cityscapes [9] and SYNTHIA [41] \rightarrow Cityscapes. For indoor, we use SceneNet [33] \rightarrow SUN [46]. Note that unlike existing literature, this work is the first to show results on the indoor setting, which depicts the generalization ability of our framework. The outdoor scene dataset has 19 categories, whereas the indoor has 13 categories. Please refer to Appendix A for more details.

Implementation Details: To have a fair comparison with the works in literature, we use the Deeplab-V2 [5] with ResNet-101 [14] as the network. We use one GPU to train our models with a batch size of 1 in all experiments. We use SGD with an initial learning rate of 2.5×10^{-4} with polynomial decay of power 0.9 [5]. We use the standard metric of mean intersection over union (mIoU) [5] to evaluate all algorithms.

Comparison with state-of-the-art: We first compare our method with state-of-the-art in literature in Table 7 for GTA5 \rightarrow Cityscapes, in Table 8 for SYNTHIA \rightarrow Cityscapes, and

Table 1. Results of adapting GTA5 to Cityscapes. The top group are methods which use source data during adaptation, while the bottom two row groups do not use any source data to adapt. Note that the middle row group use DeepLabv3+ResNet-50 as their backbone while all other methods use DeepLabv2+ResNet-101.

Source	Method	Stuff	Things	mIoU
Yes	AdaptOutput [50]	52.2	33.6	41.4
	AdvEnt [54]	57.0	37.1	45.5
	SSF-DAN [12]	57.4	36.7	45.4
	BDL [25]	61.7	38.9	48.5
	CAG [63]	61.2	42.0	50.2
	WeakDA [39]	61.0	38.8	48.2
	Stuff [56]	62.1	39.9	49.2
	FDA [59]	60.3	43.2	50.4
	SAC [1]	64.3	46.1	53.8
No	SFDA [28]	56.7	33.3	43.2
No	No Adapt.	45.6	31.6	37.5
	URMA [42]	60.3	34.0	45.1
	LD [61]	60.1	34.9	45.5
	Ours	59.0	41.3	48.8

Table 2. Results of adapting SYNTHIA to Cityscapes. The top group are methods which use source data to adapt, while the bottom two row groups do not use source data to adapt. mIoU and mIoU* are averaged over 16 and 13 categories. Note that the middle row group use DeepLabv3+ResNet-50 as the backbone while all other methods use DeepLabv2+ResNet-101. Stuff and Things mIoU is computed over the 13 categories for which all works report.

Source	Method	Stuff	Things	mIoU	mIoU*
Yes	AdaptOutput [50]	70.8	30.4	39.5	45.9
	AdvEnt [54]	74.4	31.5	41.2	48.0
	SSF-DAN [12]	74.6	34.6	-	50.0
	CAG [63]	73.9	37.4	44.5	51.4
	WeakDA [39]	78.5	35.3	44.3	51.9
	Stuff [56]	73.9	38.5	-	52.1
	FDA [59]	66.4	43.8	-	52.5
	SAC [1]	79.7	46.5	52.6	59.3
No	SFDA [28]	76.8	26.5	39.2	45.9
No	No Adapt.	57.0	23.9	32.1	36.7
	URMA [42]	64.9	32.6	39.6	45.0
	LD [61]	70.0	37.7	42.6	50.1
	Ours	69.7	37.9	43.7	50.2

SceneNet \rightarrow SUN in Table 3. Due to limited space, instead of presenting the category-wise performances, we club them into COCO-style Stuff and Things in Table 7 and 8, and present the category-wise results in appendix (Table 7 and

Table 3. Results of adapting SceneNet to SUN. The top row group does not use any source data to adapt, while the bottom row uses full supervision on the target images.

Method	bed	books	ceiling	chair	floor	furniture	objects	picture	sofa	table	tv	wall	window	mIoU
No Adapt.	19.6	10.1	22.2	42.5	65.4	21.3	13.4	20.9	18.2	27.1	6.2	57.1	20.2	26.5
Ours	35.3	23.5	34.1	48.7	73.6	26.7	11.1	29.9	36.9	38.1	15.0	63.2	27.2	35.6
Full Supervision	53.1	32.6	54.0	60.0	82.4	35.1	33.4	43.2	45.7	52.7	36.8	72.0	46.8	49.8

Table 8). Stuff includes road, sidewalk, building, wall, fence, veg, terrain and sky; while Things include sign, person, rider, car, truck, bus, train, mbike, bike, light and pole. “No Adapt.” means applying the source model directly on the target data, without adaptation. Also, as this is the first work which presents domain adaptation results on SceneNet \rightarrow SUN, we include the result with full-supervision on the target, in Table 3. As we can see, our method performs much better than “No Adapt.”, and is only a few points short of the state-of-the-art methods which use source data for adaptation.

From the tables we can also see that, our method outperforms other source-free adaptation methods, even with just using a batch size of 1, whereas some baselines use batch size > 1 to train. Our method is also comparable to many recent methods, which use source data to adapt. Most methods in literature perform an alignment either in the input or output space between the source and target domain, which not only requires the source data, but also additional models (discriminators), which are trained simultaneously. Compared to that, our framework is quite light-weight as it just involves pseudo-label training along with certain constraints.

Ablation study of transforms: In this experiment, we analyse the effect of transforms we use in our framework and the effect of learning from collage images. We use two spatial transforms, Mirror and Rotate and two augment transforms, Gaussian filter and Cutout. The results are presented in Table 4. We evaluate the model by adding only one transform at a time. As can be seen, the transforms individually improve the performance beyond just pseudo-labeling. Moreover, learning from collage images also improves the performance beyond pseudo-label learning from single images. The maximum gain is achieved when we use all of the above together. We also see similar trends for other datasets as well, and present them in appendix (Table 9). It is interesting to note that augment transforms beyond a certain parameter limit do not work as well, which is intuitive, as the content of the image may change beyond what is necessary for fine segmentation. For example, in Gaussian filtering, using a filter size more than 20 does not help with an image of size 512×1024 .

Ablation study of the framework: In this experiment, we break down every part of the framework and evaluate their performance. We present the results in Table 5 for all the

Table 4. Ablation of the transformations on GTA5 \rightarrow Cityscapes.

Collage	Mirror	Rotate	Gaussian	Cutout	mIoU
✓					46.4
	✓				45.9
		✓			45.5
			✓		46.4
				✓	45.8
✓	✓	✓	✓	✓	48.8

Table 5. Ablation of loss functions and design choices.

Methods	GTA5 \rightarrow Cityscapes	SYNTHIA \rightarrow Cityscapes	SceneNet \rightarrow SUN
No Adapt.	37.5	32.1	26.5
Update Norm	41.4	35.3	27.4
Pseudo-Label (PL)	45.6	40.2	32.1
PL + soft constraints	48.2	43.1	35.0
PL + hard constraints	47.9	43.0	34.8
Uniform thresholds	47.3	41.6	31.9
Constraints using M_s	47.3	42.2	33.2
Finetuning M_s	48.6	43.3	28.9
PL + augment	43.1	39.1	33.8
Ours	48.8	43.7	35.6

datasets. When we first update the normalization parameters, the performance improves by 1 – 4%. Then using the updated network for pseudo-label training using the target images offers a further 4 – 5% improvement. Now, imposing the transform constraints using the hard and soft constraint losses as in Eqn. 9 along with the collage images further improves the performance by about 3% compared to just pseudo-labeling.

Ablation of design choices: We perform ablation of various choices involved in designing our proposed algorithm. The first one is using category-wise thresholds for pseudo-labeling, compared to uniform thresholding for all labels. To compare, we execute our framework with an uniform threshold of 0.9 for all the labels (following [25]), as mentioned in the sixth row in Table 5. We observe that using label-wise thresholding (“Ours” in Table 5) performs better by 1.5 – 4% than uniform thresholding.

In the next ablation, we study the effect of using the norm updated source model M_s instead of target model M_t in current iteration, for the constraints of Eqn. 7, 8. If we apply the transform constraints using M_s rather than M_t , then we limit its ability to improve beyond the fixed pseudo-labels, albeit with transforms applied on them. In other words, when using M_t for the constraints, the optimization process is allowed to learn the target model and self-improve in a way such that the constraints are satisfied on the final target model. This helps to improve the performance, as is evident

Table 6. Results for test-time adaptation with a single iteration of optimization at test time.

Methods	GTA5 → Cityscapes	SYNTHIA → Cityscapes	SceneNet → SUN
No Adapt.	37.5	32.1	26.5
Entropy [55]	38.4	32.6	27.3
Likelihood [35]	38.3	32.5	27.2
Ours	39.3	33.2	27.6

by comparing the seventh row in Table 5 with the last row.

Next, we investigate whether to fine-tune the source model for adaptation or train a new target model from scratch. As can be observed from the eighth row of Table 5, fine-tuning performs worse than our method where we train a new target model from scratch. Note that the learning rate and the number of training epochs are kept the same for both cases. This can be attributed to the source model being already in a local optima in the loss landscape, thus may be less influenced by the pseudo-label losses and constraints.

Finally, we use the transforms in the standard augmentation setting (but stronger than normal augments), i.e., augment the images, pseudo-label them and learn the target model using them. We use equal portion of original and augmented images, as in our method. The results are presented as “PL+augment” in Table 5, which shows that our consistency based approach performs much better. This is because the pseudo-labels are much better on the original images rather than on the augmented ones, and it is better to transform the pseudo-labeled image, rather than pseudo-labeling the transformed image.

Test Time Adaptation: To further validate the effectiveness of our consistency based self-training approach, we use it for test-time adaptation, which is recently introduced in [48]. Here, we do not even have any unlabeled target data to adapt. Instead, we use our loss to individually adapt to each test image, resetting the model back to the source model after predicting. For TTA, we do not use the collage transformations, as we adapt to a single image at a time. We show results on the episodic fully test time adaptation setting proposed by [55] where the network cannot be trained again with any additional source or target data, other than the given test image. We compare our loss function with those from recent works [35, 55] and observe that our method performs better due to its inherent ability to exploit the regularization provided by semantic segmentation as a task (Table 10). All results share the same backbone and hyper-parameters as described in implementation details. For [35], we report the best result from SLR/HLR loss variants.

Qualitative Analysis: We present a few images and their segmentation maps for visual analysis in Figure 5. We com-

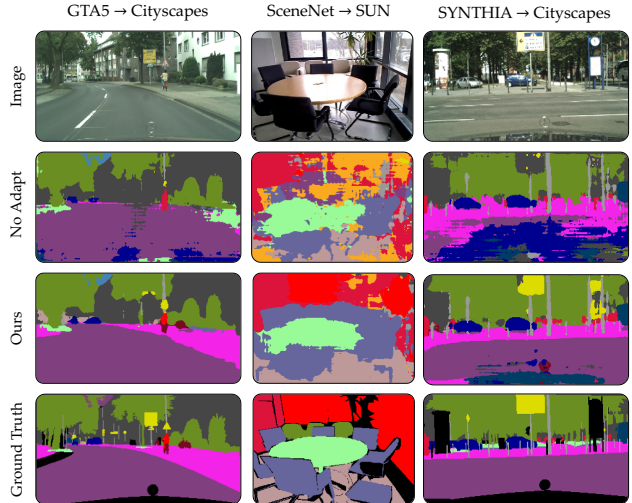


Figure 5. Examples from indoor and outdoor scenarios for visual comparison. The source→target datasets are mentioned at the top of the columns. “No Adapt” refers to using the source model directly for prediction, without any adaptation.

pare our method with “No Adapt”, i.e., directly applying the source model. As we can see in the left image, our method is able to discover one of the signs and the sidewalk, which is not segmented in “No Adapt”. For the indoor case, our method correctly segmented the glass regions as window (light red), which is segmented as picture (yellow) in “No Adapt”. In the last column, the signs are correctly discovered by our algorithm, and the road is properly segmented, while it is labeled as car (blue) in “No Adapt”. Overall, the predictions made by our method are smooth with much less noise, which can potentially be attributed to the consistency constraints. We present more examples in appendix (Figure 8).

5. Conclusion

We propose a framework for adapting semantic segmentation models from source to target without access to the labeled source data. We present a self-training framework by enforcing consistencies with certain transforms to efficiently extract information from the source model. With only a few existing works in this challenging setting, our approach compares favorably against strong baselines. Empirical evaluation shows that our method performs comparable to many state-of-the-art methods that use source data to adapt. We further show the usefulness of our approach for fully test-time adaptation in which adaptation is done individually for each test image. Future works can explore extracting information such as shape priors, from the source and infusing them into the target model, for better adaptation.

References

- [1] Nikita Araslanov and Stefan Roth. Self-supervised augmentation consistency for adapting semantic segmentation. In *CVPR*, 2021. 2, 6, 12
- [2] Konstantinos Bousmalis, Nathan Silberman, David Dohan, Dumitru Erhan, and Dilip Krishnan. Unsupervised pixel-level domain adaptation with generative adversarial networks. In *CVPR*, 2017. 2
- [3] Woong-Gi Chang, Tackgeun You, Seonguk Seo, Suha Kwak, and Bohyung Han. Domain-specific batch normalization for unsupervised domain adaptation. In *CVPR*, pages 7354–7362, 2019. 3
- [4] Wei-Lun Chang, Hui-Po Wang, Wen-Hsiao Peng, and Wei-Chen Chiu. All about structure: Adapting structural information across domains for boosting semantic segmentation. In *CVPR*, 2019. 2
- [5] Liang-Chieh Chen, George Papandreou, Iasonas Kokkinos, Kevin Murphy, and Alan L Yuille. Deeplab: Semantic image segmentation with deep convolutional nets, atrous convolution, and fully connected crfs. *TPAMI*, 2017. 1, 6
- [6] Yuhua Chen, Wen Li, and Luc Van Gool. Road: Reality oriented adaptation for semantic segmentation of urban scenes. In *CVPR*, 2018. 2
- [7] Yi-Hsin Chen, Wei-Yu Chen, Yu-Ting Chen, Bo-Cheng Tsai, Yu-Chiang Frank Wang, and Min Sun. No more discrimination: Cross city adaptation of road scene segmenters. In *ICCV*, 2017. 2
- [8] Jaehoon Choi, Taekyung Kim, and Changick Kim. Self-ensembling with gan-based data augmentation for domain adaptation in semantic segmentation. In *ICCV*, 2019. 1, 2
- [9] Marius Cordts, Mohamed Omran, Sebastian Ramos, Timo Rehfeld, Markus Enzweiler, Rodrigo Benenson, Uwe Franke, Stefan Roth, and Bernt Schiele. The cityscapes dataset for semantic urban scene understanding. In *CVPR*, 2016. 1, 6, 11
- [10] Shuyang Dai, Kihyuk Sohn, Yi-Hsuan Tsai, Lawrence Carin, and Manmohan Chandraker. Adaptation across extreme variations using unlabeled domain bridges. *BMVC*, 2020. 2
- [11] Jiahua Dong, Yang Cong, Gan Sun, Yuyang Liu, and Xiaowei Xu. Cscsl: Critical semantic-consistent learning for unsupervised domain adaptation. In *ECCV*, 2020. 2
- [12] Liang Du, Jingang Tan, Hongye Yang, Jianfeng Feng, Xiangyang Xue, Qibao Zheng, Xiaoqing Ye, and Xiaolin Zhang. Ssf-dan: Separated semantic feature based domain adaptation network for semantic segmentation. In *ICCV*, 2019. 2, 6, 12
- [13] Yaroslav Ganin, Evgeniya Ustinova, Hana Ajakan, Pascal Germain, Hugo Larochelle, François Laviolette, Mario Marchand, and Victor Lempitsky. Domain-adversarial training of neural networks. In *JMLR*, 2016. 2
- [14] Kaiming He, Xiangyu Zhang, Shaoqing Ren, and Jian Sun. Deep residual learning for image recognition. In *CVPR*, 2016. 6
- [15] Judy Hoffman, Eric Tzeng, Taesung Park, Jun-Yan Zhu, Phillip Isola, Kate Saenko, Alexei A. Efros, and Trevor Darrell. Cycada: Cycle-consistent adversarial domain adaptation. In *ICML*, 2018. 1, 2
- [16] Judy Hoffman, Dequan Wang, Fisher Yu, and Trevor Darrell. Fcns in the wild: Pixel-level adversarial and constraint-based adaptation. *CoRR*, abs/1612.02649, 2016. 1, 2
- [17] Jiaxing Huang, Shijian Lu, Dayan Guan, and Xiaobing Zhang. Contextual-relation consistent domain adaptation for semantic segmentation. In *ECCV*, 2020. 2
- [18] S. Ioffe and C. Szegedy. Batch normalization: Accelerating deep network training by reducing internal covariate shift. In *ICML*, 2015. 3
- [19] Myeongjin Kim and Hyeran Byun. Learning texture invariant representation for domain adaptation of semantic segmentation. In *CVPR*, 2020. 2
- [20] Jogendra Nath Kundu, Akshay Kulkarni, Amit Singh, Varun Jampani, and R Venkatesh Babu. Generalize then adapt: Source-free domain adaptive semantic segmentation. In *ICCV*, 2021. 3
- [21] Chen-Yu Lee, Tanmay Batra, Mohammad Haris Baig, and Daniel Ulbricht. Sliced wasserstein discrepancy for unsupervised domain adaptation. In *CVPR*, 2019. 2
- [22] Guangrui Li, Guoliang Kang, Wu Liu, Yunchao Wei, and Yi Yang. Content-consistent matching for domain adaptive semantic segmentation. In *ECCV*, 2020. 2
- [23] Rui Li, Qianfen Jiao, Wenming Cao, Hau-San Wong, and Si Wu. Model adaptation: Unsupervised domain adaptation without source data. In *CVPR*, pages 9641–9650, 2020. 2
- [24] Yanghao Li, Naiyan Wang, Jianping Shi, Jiaying Liu, and Xiaodi Hou. Revisiting batch normalization for practical domain adaptation. *ICLRW*, 2017. 3
- [25] Yunsheng Li, Lu Yuan, and Nuno Vasconcelos. Bidirectional learning for domain adaptation of semantic segmentation. In *CVPR*, 2019. 2, 6, 7, 12
- [26] Qing Lian, Fengmao Lv, Lixin Duan, and Boqing Gong. Constructing self-motivated pyramid curriculums for cross-domain semantic segmentation: A non-adversarial approach. In *ICCV*, 2019. 2
- [27] Jian Liang, Dapeng Hu, and Jiashi Feng. Do we really need to access the source data? source hypothesis transfer for unsupervised domain adaptation. In *ICML*, 2020. 2
- [28] Yuang Liu, Wei Zhang, and Jun Wang. Source-free domain adaptation for semantic segmentation. In *CVPR*, 2021. 2, 6, 12
- [29] Mingsheng Long, Yue Cao, Jianmin Wang, and Michael Jordan. Learning transferable features with deep adaptation networks. In *ICML*, 2015. 2
- [30] Mingsheng Long, Han Zhu, Jianmin Wang, and Michael I Jordan. Unsupervised domain adaptation with residual transfer networks. In *NIPS*, 2016. 2
- [31] Fengmao Lv, Tao Liang, Xiang Chen, and Guosheng Lin. Cross-domain semantic segmentation via domain-invariant interactive relation transfer. In *CVPR*, 2020. 2
- [32] John McCormac, Ankur Handa, Stefan Leutenegger, and Andrew J Davison. Scenenet rgb-d: 5m photorealistic images of synthetic indoor trajectories with ground truth. *arXiv preprint arXiv:1612.05079*, 2016. 11
- [33] John McCormac, Ankur Handa, Stefan Leutenegger, and Andrew J Davison. Scenenet rgb-d: Can 5m synthetic images beat generic imagenet pre-training on indoor segmentation? In *ICCV*, 2017. 6

- [34] Ke Mei, Chuang Zhu, Jiaqi Zou, and Shanghang Zhang. Instance adaptive self-training for unsupervised domain adaptation. *ECCV*, 2020. 2
- [35] Chaithanya Kumar Mummadi, Robin Huttmacher, Kilian Ram- bach, Evgeny Levinkov, Thomas Brox, and Jan Hendrik Metzen. Test-time adaptation to distribution shift by confidence maximization and input transformation. *arXiv preprint arXiv:2106.14999*, 2021. 2, 8, 13
- [36] Zak Murez, Soheil Kolouri, David Kriegman, Ravi Ramamoorthi, and Kyungnam Kim. Image to image translation for domain adaptation. In *CVPR*, 2018. 2
- [37] Luigi Musto and Andrea Zinelli. Semantically adaptive image-to-image translation for domain adaptation of semantic segmentation. *BMVC*, 2020. 2
- [38] Fei Pan, Inkyu Shin, Francois Rameau, Seokju Lee, and In So Kweon. Unsupervised intra-domain adaptation for semantic segmentation through self-supervision. In *CVPR*, 2020. 2
- [39] Sujoy Paul, Yi-Hsuan Tsai, Samuel Schuster, Amit K Roy-Chowdhury, and Manmohan Chandraker. Domain adaptive semantic segmentation using weak labels. *ECCV*, 2020. 2, 6, 12
- [40] Stephan R. Richter, Vibhav Vineet, Stefan Roth, and Vladlen Koltun. Playing for data: Ground truth from computer games. In *ECCV*, 2016. 1, 6, 11
- [41] German Ros, Laura Sellart, Joanna Materzynska, David Vazquez, and Antonio M. Lopez. The SYNTHIA Dataset: A large collection of synthetic images for semantic segmentation of urban scenes. In *CVPR*, 2016. 6, 11
- [42] Prabhu Teja S and Francois Fleuret. Uncertainty reduction for model adaptation in semantic segmentation. In *CVPR*, 2021. 2, 6, 12
- [43] Kuniaki Saito, Kohei Watanabe, Yoshitaka Ushiku, and Tatsuya Harada. Maximum classifier discrepancy for unsupervised domain adaptation. In *CVPR*, 2018. 2
- [44] Fatemeh Sadat Saleh, Mohammad Sadegh Aliakbarian, Mathieu Salzmann, Lars Petersson, and Jose M. Alvarez. Effective use of synthetic data for urban scene semantic segmentation. In *ECCV*, 2018. 2
- [45] Inkyu Shin, Sanghyun Woo, Fei Pan, and In So Kweon. Two-phase pseudo label densification for self-training based domain adaptation. In *ECCV*, 2020. 2
- [46] Shuran Song, Samuel P Lichtenberg, and Jianxiong Xiao. Sun rgb-d: A rgb-d scene understanding benchmark suite. In *CVPR*, 2015. 6, 11
- [47] M Naseer Subhani and Mohsen Ali. Learning from scale-invariant examples for domain adaptation in semantic segmentation. *ECCV*, 2020. 2
- [48] Yu Sun, Xiaolong Wang, Zhuang Liu, John Miller, Alexei Efros, and Moritz Hardt. Test-time training with self-supervision for generalization under distribution shifts. In *ICML*, 2020. 8
- [49] Luan Tran, Kihyuk Sohn, Xiang Yu, Xiaoming Liu, and Manmohan Chandraker. Gotta adapt 'em all: Joint pixel and feature-level domain adaptation for recognition in the wild. In *CVPR*, 2019. 2
- [50] Yi-Hsuan Tsai, Wei-Chih Hung, Samuel Schuster, Kihyuk Sohn, Ming-Hsuan Yang, and Manmohan Chandraker. Learning to adapt structured output space for semantic segmentation. In *CVPR*, 2018. 1, 2, 6, 12
- [51] Yi-Hsuan Tsai, Kihyuk Sohn, Samuel Schuster, and Manmohan Chandraker. Domain adaptation for structured output via discriminative patch representations. In *ICCV*, 2019. 2
- [52] Eric Tzeng, Judy Hoffman, Kate Saenko, and Trevor Darrell. Adversarial discriminative domain adaptation. In *CVPR*, 2017. 1, 2
- [53] Dmitry Ulyanov, Andrea Vedaldi, and Victor Lempitsky. Instance normalization: The missing ingredient for fast stylization. *arXiv preprint arXiv:1607.08022*, 2016. 3
- [54] Tuan-Hung Vu, Himalaya Jain, Maxime Bucher, Matthieu Cord, and Patrick Pérez. Advent: Adversarial entropy minimization for domain adaptation in semantic segmentation. In *CVPR*, 2019. 2, 6, 12
- [55] Dequan Wang, Evan Shelhamer, Shaoteng Liu, Bruno Olshausen, and Trevor Darrell. Tent: Fully test-time adaptation by entropy minimization. In *ICLR*, 2021. 2, 8, 13
- [56] Zhonghao Wang, Mo Yu, Yunchao Wei, Rogerio Feris, Jinjun Xiong, Wen-mei Hwu, Thomas S Huang, and Honghui Shi. Differential treatment for stuff and things: A simple unsupervised domain adaptation method for semantic segmentation. In *CVPR*, 2020. 2, 6, 12
- [57] Zuxuan Wu, Xintong Han, Yen-Liang Lin, Mustafa Gkhan Uzunbas, Tom Goldstein, Ser Nam Lim, and Larry S. Davis. Dcan: Dual channel-wise alignment networks for unsupervised scene adaptation. In *ECCV*, 2018. 2
- [58] Haifeng Xia, Handong Zhao, and Zhengming Ding. Adaptive adversarial network for source-free domain adaptation. In *ICCV*, 2021. 2
- [59] Yanchao Yang and Stefano Soatto. Fda: Fourier domain adaptation for semantic segmentation. In *CVPR*, 2020. 2, 6, 12
- [60] Hao-Wei Yeh, Baoyao Yang, Pong C Yuen, and Tatsuya Harada. Sofa: Source-data-free feature alignment for unsupervised domain adaptation. In *WACV*, 2021. 2
- [61] Fuming You, Jingjing Li, Lei Zhu, Zhi Chen, and Zi Huang. Domain adaptive semantic segmentation without source data. In *ACM-MM*, 2021. 3, 6, 12
- [62] Hongyi Zhang, Moustapha Cisse, Yann N Dauphin, and David Lopez-Paz. mixup: Beyond empirical risk minimization. *ICLR*, 2017. 5
- [63] Qiming Zhang, Jing Zhang, Wei Liu, and Dacheng Tao. Category anchor-guided unsupervised domain adaptation for semantic segmentation. *NeurIPS*, 2019. 2, 6, 12
- [64] Yang Zhang, Philip David, and Boqing Gong. Curriculum domain adaptation for semantic segmentation of urban scenes. In *ICCV*, 2017. 2
- [65] Yiheng Zhang, Zhaofan Qiu, Ting Yao, Dong Liu, and Tao Mei. Fully convolutional adaptation networks for semantic segmentation. In *CVPR*, 2018. 2
- [66] Yang Zou, Zhiding Yu, B. V. K. Vijaya Kumar, and Jinsong Wang. Domain adaptation for semantic segmentation via class-balanced self-training. In *ECCV*, 2018. 2

Appendix A. Datasets

GTA5 → Cityscapes: In this setting, we consider GTA5 [40] as the source and Cityscapes [9] as the target dataset. The source images are at 760×1280 resolution, while the target images are used at 512×1024 . The datasets have 19 categories. The source dataset has 24966 training images and the target has 2975 training images on which we perform adaptation, and 500 validation images. We report the performance on these 500 validation images as is the usual practice in the literature.

SYNTHIA → Cityscapes: In this setting, we consider SYNTHIA [41] as the source and Cityscapes [9] as the target dataset. SYNTHIA contains 9400 training images. However, unlike GTA5, due to lack of proper annotations for a few categories in SYNTHIA, we remove them from evaluation and report the results for 16 categories, following the literature.

SceneNet → SUN: Both of the above two settings are for outdoor scenes, and in this setting we consider indoor scenes with SceneNet [32] as the source and SUN [46] as the target. The SceneNet dataset has around 5 million simulated images. However, a lot of the images are rather simple with only a few categories in them. Thus, to train the source model, we only choose the top 50,000 images having the highest number of categories. The SUN dataset contains 5285 training images on which we perform adaptation and 5050 test images which are used for evaluation. Both of these datasets contain 13 categories. Specifically, we use the label transformation available with the SceneNet dataset¹ to map the labels in the SUN dataset such that it matches with the label space of SceneNet.

Appendix B. Category-wise Segmentation Results

In this section, we present the category-wise segmentation results for the two dataset settings, GTA5→Cityscapes and SYNTHIA→Cityscapes in Table 7 and 8 respectively.

Appendix C. Hyper-parameter analysis of cutout

In this section, we analyse the effect of the hyperparameters involved in the cutout transformation. Recall from the paper, in this transformation, we choose two parameters: size b of the square block, and the percentage p of the image to be removed. Given these two parameters, we choose the number of blocks to be removed as $k = \frac{pHW}{b^2}$. We execute our framework for various values of b and p , while keeping the rest of the framework same, and present the performance obtained in Figure 6. By using

¹<https://github.com/ankurhanda/sunrgbd-meta-data>

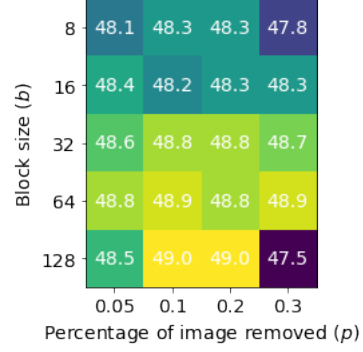


Figure 6. Ablation study of the cutout transformation.

this transform, we want the network to learn rich context information, while performing inpainting in the output space. As can be seen, with lower block size and higher percentage of image removed, the performance degrades. This is because by doing so the image becomes noisy, rather than structured removal, i.e., removed portions become well distributed throughout the image, which makes it harder to learn context information. However, with higher block size, and moderate percentage of image removed, the performance increases. We choose $b = 64, p = 0.2$, in our experiments on outdoor images, where the resolution of the image is high, and we choose $b = 32, p = 0.1$, for indoor experiments, with lower image sizes.

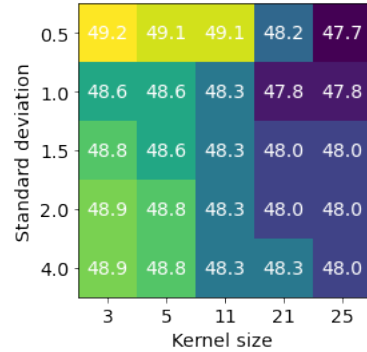


Figure 7. Ablation study of the Gaussian filtering transformation.

Appendix D. Hyper-parameter analysis of Gaussian filter

In this section, we analyse the effect of two hyperparameters in the Gaussian filter transformation. The two hyperparameters are the kernel size and the standard deviation of the filter. Instead of keeping a single standard deviation for the filter, we choose it randomly between $[0.1, \sigma_{max}]$, where σ_{max} is the hyper-parameter to choose. The image becomes more blurry with higher kernel size and lower standard deviation.

Table 7. Results of adapting GTA5 to Cityscapes. The top row group are methods which use source data during adaptation, while the bottom row group do not use any source data to adapt. Note that the middle row group use DeepLabv3+ResNet-50 as their backbone while all other methods use DeepLabv2+ResNet-101.

Source	Method	road	sidewalk	building	wall	fence	pole	light	sign	veg	terrain	sky	person	rider	car	truck	bus	train	mbike	bike	mIoU
Yes	AdaptOutput [50]	86.5	25.9	79.8	22.1	20.0	23.6	33.1	21.8	81.8	25.9	75.9	57.3	26.2	76.3	29.8	32.1	7.2	29.5	32.5	41.4
	AdvEnt [54]	89.4	33.1	81.0	26.6	26.8	27.2	33.5	24.7	83.9	36.7	78.8	58.7	30.5	84.8	38.5	44.5	1.7	31.6	32.4	45.5
	SSF-DAN [12]	90.3	38.9	81.7	24.8	22.9	30.5	37.0	21.2	84.8	38.8	76.9	58.8	30.7	85.7	30.6	38.1	5.9	28.3	36.9	45.4
	BDL [25]	91.0	44.7	84.2	34.6	27.6	30.2	36.0	36.0	85.0	43.6	83.0	58.6	31.6	83.3	35.3	49.7	3.3	28.8	35.6	48.5
	CAG [63]	90.4	51.6	83.8	34.2	27.8	38.4	25.3	48.4	85.4	38.2	78.1	58.6	34.6	84.7	21.9	42.7	41.1	29.3	37.2	50.2
	WeakDA [39]	91.6	47.4	84.0	30.4	28.3	31.4	37.4	35.4	83.9	38.3	83.9	61.2	28.2	83.7	28.8	41.3	8.8	24.7	46.4	48.2
	Stuff [56]	90.6	44.7	84.8	34.3	28.7	31.6	35.0	37.6	84.7	43.3	85.3	57.0	31.5	83.8	42.6	48.5	1.9	30.4	39.0	49.2
	FDA [59]	92.5	53.3	82.3	26.5	27.6	36.4	40.5	38.8	82.2	39.8	78.0	62.6	34.4	84.9	34.1	53.1	16.8	27.7	46.4	50.4
	SAC [1]	90.4	53.9	86.6	42.4	27.3	45.1	48.5	42.7	87.4	40.1	86.1	67.5	29.7	88.5	49.1	54.6	9.8	26.6	45.3	53.8
No	SFDA [28]	84.2	39.2	82.7	27.5	22.1	25.9	31.1	21.9	82.4	30.5	85.3	58.7	22.1	80.0	33.1	31.5	3.6	27.8	30.6	43.2
No	No Adapt.	79.7	21.8	66.8	19.3	20.6	22.8	28.9	12.9	76.3	19.5	60.9	56.2	26.6	77.8	33.3	27.7	3.9	25.0	32.5	37.5
	URMA [42]	92.3	55.2	81.6	30.8	18.8	37.1	17.7	12.1	84.2	35.9	83.8	57.7	24.1	81.7	27.5	44.3	6.9	24.1	40.4	45.1
	LD [61]	91.6	53.2	80.6	36.6	14.2	26.4	31.6	22.7	83.1	42.1	79.3	57.3	26.6	82.1	41.0	50.1	0.3	25.9	19.5	45.5
	Ours	89.2	37.3	82.4	29.0	23.5	31.8	34.6	28.7	84.8	45.5	80.2	62.6	32.6	86.1	45.6	43.8	0.0	34.6	54.4	48.8

Table 8. Results of adapting SYNTHIA to Cityscapes. The top group are methods which use source data during adaptation, while the bottom row group do not use any source data to adapt. mIoU and mIoU* are averaged over 16 and 13 categories. Note that the middle row group use DeepLabv3+ResNet-50 as their backbone while all other methods use DeepLabv2+ResNet-101.

Source	Method	road	sidewalk	building	wall	fence	pole	light	sign	veg	sky	person	rider	car	bus	mbike	bike	mIoU	mIoU*
Yes	AdaptOutput [50]	79.2	37.2	78.8	10.5	0.3	25.1	9.9	10.5	78.2	80.5	53.5	19.6	67.0	29.5	21.6	31.3	39.5	45.9
	AdvEnt [54]	85.6	42.2	79.7	8.7	0.4	25.9	5.4	8.1	80.4	84.1	57.9	23.8	73.3	36.4	14.2	33.0	41.2	48.0
	SSF-DAN [12]	84.6	41.7	80.8	-	-	-	11.5	14.7	80.8	85.3	57.5	21.6	82.0	36.0	19.3	34.5	-	50.0
	CAG [63]	84.7	40.8	81.7	7.8	0.0	35.1	13.3	22.7	84.5	77.6	64.2	27.8	80.9	19.7	22.7	48.3	44.5	51.4
	WeakDA [39]	92.0	53.5	80.9	11.4	0.4	21.8	3.8	6.0	81.6	84.4	60.8	24.4	80.5	39.0	26.0	41.7	44.3	51.9
	Stuff [56]	83.0	44.0	80.3	-	-	-	17.1	15.8	80.5	81.8	59.9	33.1	70.2	37.3	28.5	45.8	-	52.1
	FDA [59]	79.3	35.0	73.2	-	-	-	19.9	24.0	61.7	82.6	61.4	31.1	83.9	40.8	38.4	51.1	-	52.5
	SAC [1]	89.3	47.2	85.5	26.5	1.3	43.0	45.5	32.0	87.1	89.3	63.6	25.4	86.9	35.6	30.4	53.0	52.6	59.3
No	SFDA [28]	81.9	44.9	81.7	4.0	0.5	26.2	3.3	10.7	86.3	89.4	37.9	13.4	80.6	25.6	9.6	31.3	39.20	45.9
No	No Adapt.	37.6	18.7	73.8	9.95	0.1	26.4	8.9	13.9	74.7	80.4	52.4	16.1	39.2	21.9	13.2	25.8	32.1	36.7
	URMA [42]	59.3	24.6	77.0	14.0	1.8	31.5	18.3	32.0	83.1	80.4	46.3	17.8	76.7	17.0	18.5	34.6	39.6	45.0
	LD [61]	77.1	33.4	79.4	5.8	0.5	23.7	5.2	13.0	81.8	78.3	56.1	21.6	80.3	49.6	28.0	48.1	42.6	50.1
	Ours	74.3	33.7	78.9	14.6	0.7	31.5	21.3	28.8	80.2	81.6	50.7	24.5	78.3	11.6	34.4	53.7	43.7	50.2

tion. As the image becomes more blurry, it becomes difficult for the network to figure out the content, and thus we see a degradation in performance in the top right corner in Figure 7. Note that the standard deviation mentioned in the figure signify σ_{max} . We use a kernel size of 5 and $\sigma_{max} = 2$.

Appendix E. Ablation of the transformations

Here, we perform ablation of the four transformations used in our framework - mirror, rotate, gaussian filter and cutout. In the paper, we presented results on GTA5 \rightarrow Cityscapes (Table 4), and here we present on the other two settings, i.e., SYNTHIA \rightarrow Cityscapes and SceneNet \rightarrow SUN. As can be seen in Table 9, each of the transformations have their own contribution towards the final performance,

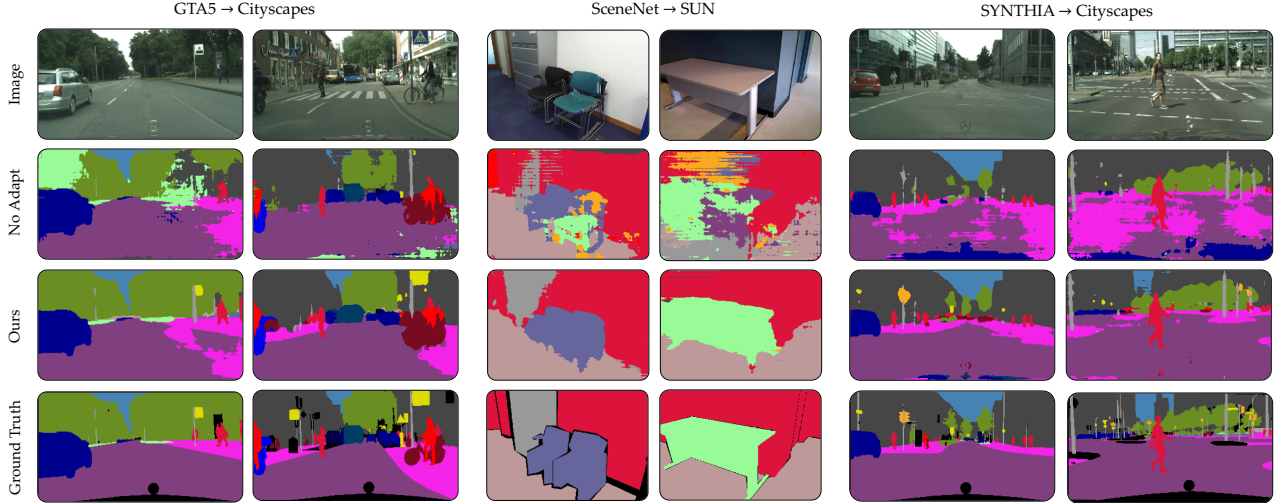


Figure 8. Qualitative visualization. The first two columns and the last two columns show results on outdoor scenes, while the middle two columns show results on indoor scenes.

Table 9. Ablation of the transformations.

Collage	Mirror	Rotate	Gaussian	Cutout	SYNTHIA → Cityscapes	SceneNet → SUN
✓					40.4	32.2
	✓				41.9	34.6
		✓			42.3	34.8
			✓		42.5	34.5
				✓	41.9	33.1
✓	✓	✓	✓	✓	43.7	35.6

however, an ensemble of all the transformation performs the best.

Appendix F. Additional test time adaptation results

In this section, we present additional results for the fully test time adaptation setting, where we optimize the network for 5 iterations using the given loss functions per single test image. Note that although not designed specifically for test time adaptation, our consistency based approach is able to perform good on this task as well. As can be seen in Table 10, we perform better or within a close margin to the loss functions proposed by previous works [35, 55] which were completely dedicated towards solving the test time adaptation problem.

Appendix G. Qualitative Analysis

In Figure 8 we present a visual comparison of our method with directly applying the source model on the target images,

Table 10. Results for test-time adaptation with a single or five iterations of optimization at test time.

Methods	GTA5 → Cityscapes	SYNTHIA → Cityscapes	SceneNet → SUN
No Adapt.	37.6	32.1	26.5
1 Iteration			
Entropy [55]	38.4	32.6	27.3
Likelihood [35]	38.3	32.5	27.2
Ours	39.3	33.2	27.6
5 Iterations			
Entropy [55]	40.4	34.0	28.8
Likelihood [35]	39.4	33.7	27.9
Ours	42.2	36.0	28.4

shown as “No Adapt”. As can be seen in the first column, our method is able to properly label the signs, even though the source model does not have them, as shown in “No Adapt”.

Similar discussions can be extended to results in the second column. In the third and fourth columns, the source model is very confused with the shadows on the chairs and tables, and assigns them multiple labels. However, our method is able to predict the accurate labels with proper segmentation. In the last column, the network mistakes most portion of the road as sidewalk, a prior that pedestrians can be more often seen on sidewalks than roads. However, our method is able segment the road and sidewalk properly and is also able to segment a few of the road signs in the background.